

## Femtonewton Force Spectroscopy of Single Extended DNA Molecules

Jens-Christian Meiners and Stephen R. Quake

*Department of Applied Physics, California Institute of Technology, Pasadena, California 91125*

(Received 27 December 1999)

We studied the thermal fluctuations of single DNA molecules with a novel optical tweezer based force spectroscopy technique. This technique combines femtonewton sensitivity with millisecond time resolution, surpassing the sensitivity of previous force measurements in aqueous solution with comparable bandwidth by a hundredfold. Our data resolve long-standing questions concerning internal hydrodynamics of the polymer and anisotropy in the molecular relaxation times and friction coefficients. The dynamics at high extension show interesting nonlinear behavior.

PACS numbers: 87.15.Ya, 05.40.Jc, 36.20.Ey

Single molecule force spectroscopy has become a valuable tool to study the intramolecular forces involved in unfolding a protein [1,2] or inducing conformational changes in a polymer [3]. These chemical forces are typically of the order of tens of piconewtons and can readily be measured with atomic force microscope techniques. Entropic forces as low as 100 fN have been measured with optical and magnetic traps [4–6], but thermal motion of the force-transducing latex bead in the trap limits the time resolution of these techniques and allows dynamic measurements only for piconewton force fluctuations [7,8]. We have developed a scheme using dual optical tweezer force sensors that overcomes this limitation by making a cross-correlated heterodyne measurement. The thermal motions of the two beads are independent and uncorrelated, allowing us to measure the correlations introduced by a molecule whose ends are attached to the beads. Thus, one can measure the dynamic motion of the molecule with high temporal and force resolution by computing the cross correlation between the measured forces acting on the two beads. This femtonewton force spectroscopy (FFS) scheme is general and can in principle be adapted to make high-resolution measurements of the average power stroke of molecular motors such as myosin, kinesin, and RNA polymerase. It is superior to measuring individual events [8,9] or the instantaneous cross correlation [10] since it effectively self-averages over the entire period of the measurement, giving a concomitant improvement in the signal-to-noise ratio and removing human bias in separating true events from noise fluctuations.

We used FFS to study the thermal fluctuations of a single DNA molecule. DNA has proved to be a useful model system to study the complex dynamic behavior of polymers, an intriguing subject of long-standing theoretical and experimental interest. An important application of polymer dynamics has been to understand the behavior of polymers in hydrodynamic flow, where one observes fascinating effects such as drag reduction in turbulent pipe flow. To help understand this problem, many years ago De Gennes predicted that polymers would exhibit a “coil stretch” phase transition in extensional flow [11]. Theoretical arguments and experiments have shown that the critical fluid strain

rate at which polymers extend is  $\dot{\epsilon} \approx 1/\tau$ , where  $\tau$  is the fundamental relaxation time of the polymer. Subtle hysteresis effects are possible according to how  $\tau$  depends on extension.

In addition to the practical reasons to investigate extended polymer dynamics, there are also fundamental questions about the equilibrium dynamics of a polymer. For example, it has been predicted that due to symmetry breaking  $\tau$  will “split” into distinct longitudinal and transverse components as the polymer is extended. Two potential contributions have been identified: geometric effects due to the nonlinear spring constant [12], and an alignment effect due to anisotropic friction coefficients [13,14]. Another historically important example is the notion that internal hydrodynamic effects should cause the polymer’s friction coefficient to increase as it extends, causing it to go from a “non-free-draining” state to a “free-draining” state. It has been suggested that this would be the dominant effect on  $\tau$ , which would then also increase [11,13]. However, there is little direct experimental evidence about  $\tau$  or even the behavior of the friction coefficient. One study of DNA in extensional flow provided indirect evidence that the molecule does not become free draining up to 80% extension [15], but subsequent theoretical interpretations of the experiment are conflicting [16–19]. Another study with DNA extended up to 80% with optical tweezers showed that the internal modes are related by a power law whose exponent is an intermediate value between the free-draining and non-free-draining predictions [20]. The data from that study also show that the nonlinearity of the polymer spring constant affects the transverse relaxation time [12]. Finally, it has been shown that when DNA is confined to a slit geometry, the walls screen the hydrodynamic interactions and the polymer becomes free draining [21].

We studied the behavior of 6 DNA molecules at a total of 36 different extensions ranging from 74% to 92%. The experimental system is shown schematically in Fig. 1(a). A  $\lambda$ -phage DNA molecule with beads attached to its ends is stretched with a dual-beam optical tweezer apparatus. We record the Brownian motion of the beads by imaging the scattered laser light from each sphere onto a quadrant

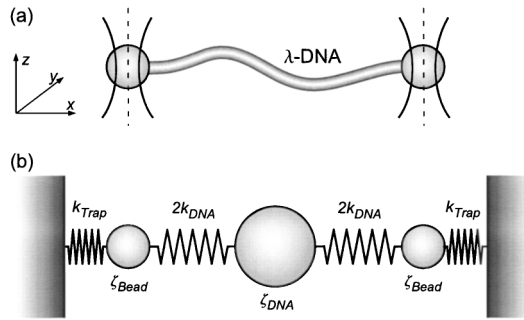


FIG. 1. Measuring the thermal fluctuations of a single DNA molecule with optical tweezers. (a) A DNA molecule of the  $\lambda$ -phage with beads attached to its ends is stretched with a dual-beam optical tweezer apparatus. We record the Brownian motion of the beads by imaging the scattered laser light from each sphere onto a quadrant photodiode. This gives a measurement of the displacement of the bead from the focus of the laser beam in the  $x$  and  $y$  direction. (b) The dynamic model used to find the spring constants and friction coefficients of the DNA molecules from the measured correlation functions. The DNA is modeled as a sphere with a friction coefficient  $\zeta_{\text{DNA}}$  and two springs, each of strength  $2k_{\text{DNA}}$ , giving an overall spring constant of  $k_{\text{DNA}}$ .

photodiode. This gives a measurement of the displacement of the bead from the focus of the laser beam in the  $x$  and  $y$  directions. In order to minimize the cross talk between the signals from the two traps, the trapping beams are orthogonally polarized and chopped alternately at a frequency of 80 kHz, and the scattered light is detected synchronously in the appropriate polarization. For each data set,  $10^7$  such position measurements were made at a rate of 20 kHz for each trap. A typical trap relaxation time was  $\tau_{\text{trap}} = 0.3$  ms, which corresponds to a spring constant of  $k_{\text{trap}} = 25$  pN/ $\mu\text{m}$ . Details of the experimental apparatus have been published elsewhere [22]. The DNA-bead complexes were prepared by labeling  $\lambda$ -DNA at either end with biotin and digoxigenin (dig), respectively [23]. Monoclonal dig antibodies from mouse cells (Roche) were bound to the dig-labeled DNA end. This DNA-antibody complex was incubated over night with equal amounts of goat antimouse IgG-coated (where IgG denotes immunoglobulin in type G) beads (polysciences) and streptavidin-coated beads (Bangs Laboratories), both 1  $\mu\text{m}$  in diameter. A threefold excess of DNA over beads was used in order to compensate for incomplete labeling and binding. Finally, the bead-DNA-bead complexes were diluted in 10 mM NaCl-TE buffer (10 mM TrisCl, 1 mM EDTA, 10 mM NaCl, pH 8.0) to a volume fraction of  $\phi = 10^{-6}$ . This solution was hermetically sealed in a 100  $\mu\text{m}$  deep sample cell. Measurements were taken while the DNA was held at a depth of 15  $\mu\text{m}$ , and the absolute distance between the centers of the beads was measured for each data set by video microscopy.

From this time-resolved measurement of the forces acting onto the beads the correlation functions  $\langle f_1(t)f_1(0) \rangle$ ,

$\langle f_2(t)f_2(0) \rangle$ , and  $\langle f_1(t)f_2(0) \rangle$  were computed. The auto-correlation functions fit an exponential

$$\langle f_i(t)f_i(0) \rangle = k_a k_B T e^{-t/\tau_a}, \quad (1)$$

yielding the spring constant  $k_a$  and time constant  $\tau_a$  of the relaxation of the beads in their traps. Similarly, the end-to-end cross-correlation function of the polymer fluctuations can be described by a stretched exponential

$$\langle f_1(t)f_2(0) \rangle = k_c k_B T e^{-(t/\tau_c)^\nu}, \quad (2)$$

where  $k_c$  is a spring constant,  $\tau_c$  a relaxation time, and  $\nu$  a stretch exponent [24]. Hydrodynamic coupling between the beads contributes an additional fast-decaying term to the correlation function, which is well understood from earlier work [22]. This hydrodynamic interaction gives rise to the pronounced dip that is seen in the correlation functions (Fig. 2) during the first millisecond for smaller extensions. In the absence of the DNA molecule it is described by

$$h(t) = e^{-(1+\varepsilon_i)t/\tau} - e^{-(1-\varepsilon_i)t/\tau}, \quad (3)$$

with  $\varepsilon_x = 3a/2D$  longitudinally and  $\varepsilon_{y,z} = 3a/2D$  in the transverse directions, where  $a$  and  $D$  denote the radius and the separation of the beads, respectively. The presence of the DNA screens this hydrodynamic coupling between the end spheres to about 60% of its native amplitude.

The measured relaxation times and spring constants are shown in Figs. 3(a) and 3(b). We fixed the exponent

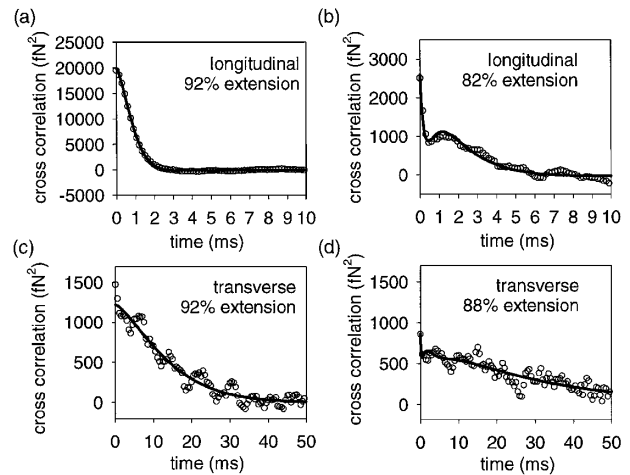


FIG. 2. Relaxation of a single, extended DNA molecule as revealed by the cross correlation between the forces acting onto the end beads. Panels (a) and (b) show the longitudinal relaxation of a molecule that is extended to 92% and 82% of its contour length, respectively. Only every third data point is plotted. Panels (c) and (d) show the transverse relaxation at 92% and 88%, respectively, with every tenth data point being plotted in the graph. A stretched single exponential decay has been fitted to all data sets, with an additional correction for the hydrodynamic interactions between the beads. This hydrodynamic interaction gives rise to the pronounced dip that is seen in the correlation functions during the first millisecond for smaller extensions. The ultimate force sensitivity of the apparatus is 6 fN rms.

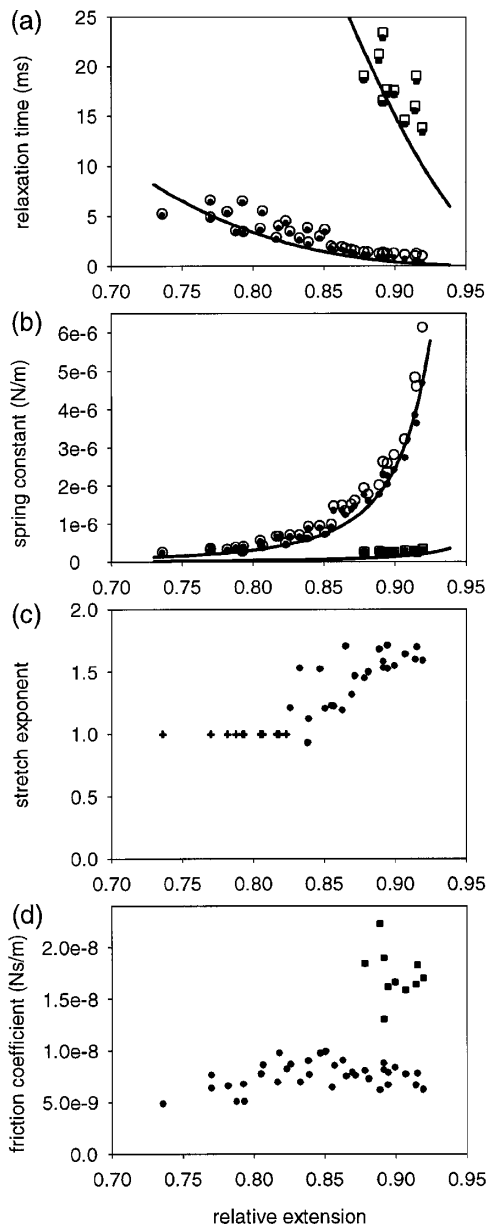


FIG. 3. Thermal fluctuations of a DNA molecule as a function of its extension, compiled from measurements on six different molecules. Experimental data points in the longitudinal direction are indicated as circles, and square mark the transverse data points. Uncorrected data from the fits are shown as open symbols, and the corrected data points are shown as the filled symbols. (a) The relaxation times of the DNA-dumbbell as a function of extension as determined from the least-square fits to Eq. (2) as well as the corrected relaxation times from Eq. (4). The solid lines indicate the predictions from the simple modified Rouse model [12] in Eq. (5). (b) The longitudinal and transverse spring constants of the molecule, as determined from the amplitude of the fluctuations, as well as the corrected values accounting for the finite stiffness of the optical traps. The predictions of the wormlike chain model for both directions are indicated as solid lines. (c) The stretch exponent  $\nu$  for the thermal relaxation of the polymer. The fitted values of  $\nu$  are shown above 82% extension. Below 82%, it was not necessary to let  $\nu$  be a free parameter in the fits. (d) The friction coefficient of the DNA molecule as a function of its extension.

$\nu = 1$  when fitting the data at lower extensions. However, above 82% there were clear systematic errors in the fits, and the simple exponential decay deviated from the data both at short and long time scales. This behavior does not appear to be due to higher order Rouse-Zimm modes, since those modes would be even more evident at lower extension where the time resolution is better. Nevertheless, we modified Eq. (2) to include various models of higher order mode structures with a single new parameter, and found that the fits still exhibited systematic errors. Adding enough free parameters led to good fits, but the values of the fitted parameters were inconsistent with known [20] or expected [24] features of the mode structure. We then returned to Eq. (2) and allowed  $\nu$  to be fit as a free parameter, and found that the fits were free of obvious systematic errors. The fitted parameter  $\nu$  increased from 1.0 to 1.6 as the extension increased [Fig. 3(c)]. While such superexponential relaxation is well known in Levi-flight-like anomalous diffusion problems [25], we can only speculate about its physical origin in the present situation. Possible causes might include mode mixing in the polymer, perhaps due to sequence heterogeneity or the highly nonlinear spring constant, or complex dynamic effects due to transition force-assisted denaturation.

If  $k_{\text{trap}} \gg k_{\text{DNA}}$  and  $\tau_{\text{trap}} \ll \tau_{\text{DNA}}$ , then the fitted parameters from above are  $k_c = k_{\text{DNA}}$ ,  $\tau_c = \tau_{\text{DNA}}$ ,  $k_a = k_{\text{trap}}$ , and  $\tau_a = \tau_{\text{trap}}$ . However, as either the spring constant or relaxation time of the DNA approaches that of the trap, there will be mixing in the measured values from the cross- and autocorrelations. It is straightforward to solve the dumbbell-like model system outlined in Fig. 1(b) and show that the corrections are

$$k_{\text{DNA}} = k_c \frac{\zeta_{\text{bead}}}{\tau_a(k_a + k_c)}, \quad (4)$$

$$\tau_{\text{DNA}} = \tau_c \frac{k_a(1 - \tau_a/\tau_c) - k_c(1 + \tau_a/\tau_c)}{(k_a + k_c)(1 - \tau_a/\tau_c)}.$$

These corrections are negligible at the smallest extensions, but become significant when the spring constant of the DNA increases. For comparison both the raw, uncorrected data and the corrected values for the relaxation times and spring constants are shown in Figs. 3(a) and 3(b), along with the predicted values from theoretical calculations. The uncorrected as well as the corrected data show a clear trend towards higher spring constants and shorter relaxation times as the extension increases, as well as a marked anisotropy. In fact, the corrected longitudinal spring constant derived from Eqs. (1), (2), and (4) increases rapidly from 0.2 pN/ $\mu\text{m}$  at 74% extension to 4.7 pN/ $\mu\text{m}$  at 92% extension [Fig. 3(b)], while the transverse spring constant reaches only 0.3 pN/ $\mu\text{m}$  at 92% extension. This behavior is in good agreement with the predictions from the wormlike chain model [12], which yields for the longitudinal and transverse spring constants of an extended polymer  $k_{\text{DNA},\parallel} = (dF/dx)|_E$  and  $k_{\text{DNA},\perp} = F(E)/E$ , where  $F(x)$

is the force-extension relationship of a wormlike chain [18],  $F(x) = (k_B T/l_p) [\frac{1}{4}(1 - x/L_0)^{-2} - \frac{1}{4} + x/L_0]$ , and  $E$  the end-to-end distance of the polymer. Using a persistence length  $l_p$  of 53 nm, a least-square fit for the longitudinal spring constant indicates a contour length  $L_0$  of approximately  $16.1 \pm 0.2 \mu\text{m}$ , which is somewhat below the crystallographic contour length of the DNA molecule of  $16.4 \mu\text{m}$ . This 2% discrepancy might be caused by steric effects at the anchor points of the DNA as well as uncertainties in the calibration of the video microscope and the bead diameter.

The relaxation times of the DNA are remarkably well described by the same model if the longitudinal and transverse friction coefficients of the DNA are assumed to be those of a rigid rod with the dimensions of the molecule, i.e., a length of  $16.4 \mu\text{m}$  and a diameter  $d$  of 2.5 nm. Those relaxation times are

$$\begin{aligned} \tau_{\text{DNA},\parallel} &= \frac{2\eta L_0 l_p}{\pi k_B T \ln(L_0/d)} \left[ \frac{1}{2L_0(1 - E/L_0)^3} + \frac{1}{L_0} \right]^{-1}, \\ \tau_{\text{DNA},\perp} &= \frac{4\eta L_0 l_p}{\pi k_B T \ln(L_0/d)} \\ &\times \left[ \frac{1}{4E(1 - E/L_0)^2} - \frac{1}{4E} + \frac{1}{L_0} \right]^{-1}, \end{aligned} \quad (5)$$

and the comparison with the experimental data is shown in Fig. 3(a).

One can use the measured values of the relaxation time and spring constant to derive the DNA molecule's friction coefficient, since  $\tau_{\text{DNA}} \propto \zeta_{\text{DNA}}/k_{\text{DNA}}$ , where  $\zeta_{\text{DNA}}$  denotes the dynamic friction coefficient of the polymer chain and will take on distinct values for the longitudinal and transverse directions. A proportionality factor is needed to ensure that this definition of  $\zeta_{\text{DNA}}$  is consistent with the fluctuation-dissipation theorem [24]. Its numerical value is 0.25 in the dumbbell-like model [Fig. 1(b)], and  $1/\pi^2$  in a continuum model. The measured friction coefficients are independent of extension over the measured range [Fig. 3(d)] and in the longitudinal direction  $\zeta_{\text{DNA},\parallel} = 7.6(0.2) \times 10^{-9} \text{ N s/m}$ , while in the transverse direction  $\zeta_{\text{DNA},\perp} = 17.3(0.8) \times 10^{-9} \text{ N s/m}$ . The ratio of transverse to longitudinal is 2.28 (0.12), close to the expected value of 2 and clearly distinct from unity. The given errors are statistical and do not include uncertainties in the numerical prefactor in our dynamic model, which can at least in part account for the fact that the measured absolute values are 25% and 15% smaller than the predicted values of the friction coefficients of a rigid rod whose dimensions are comparable to the DNA molecule.

In conclusion, we have used FFS to study the dynamics of an extended polymer and measured the anisotropy of the longitudinal and transverse relaxation times. We show that this effect is due to anisotropy in both the friction coefficient and spring constant, from hydrodynamic and geo-

metric effects, respectively. The anisotropy in the friction coefficient is consistent with rodlike (or freely draining) hydrodynamic behavior. The fact that the fundamental relaxation time  $\tau$  decreases as a function of extension shows that hysteresis is unlikely in the coil-stretch transition, and will also serve to broaden the transition. The correlation functions show superexponential relaxation at high extensions, which may indicate the presence of interesting new physics.

This work was supported by the National Science Foundation CAREER program.

- 
- [1] M. Rief, M. Gautel, F. Oesterhelt, J.M. Fernandez, and H.E. Gaub, *Science* **276**, 1109 (1997).
  - [2] M.S.Z. Kellermayer, S.B. Smith, H.L. Granzier, and C. Bustamante, *Science* **276**, 1112 (1997).
  - [3] M. Rief, F. Oesterhelt, B. Heymann, and H.E. Gaub, *Science* **275**, 1295 (1997).
  - [4] M.D. Wang, H. Yin, R. Landick, J. Gelles, and S.M. Block, *Biophys. J.* **72**, 1335 (1997).
  - [5] S.B. Smith, L. Finzi, and C. Bustamante, *Science* **258**, 1122 (1992).
  - [6] T.R. Strick, J.-F. Allemand, D. Bensimon, A. Bensimon, and V. Croquette, *Science* **271**, 1835 (1996).
  - [7] T.J. Finer, R.M. Simmons, and J.A. Spudich, *Nature (London)* **368**, 113 (1994).
  - [8] K. Svoboda, C.F. Schmidt, B.J. Schnapp, and S.M. Block, *Nature (London)* **365**, 721 (1993).
  - [9] S.M. Block, *Nature (London)* **378**, 132 (1995).
  - [10] A.D. Metha, T.J. Finer, and J.A. Spudich, *Proc. Natl. Acad. Sci. U.S.A.* **94**, 7927 (1997).
  - [11] P.G. De Gennes, *J. Chem. Phys.* **60**, 5030 (1974).
  - [12] J.W. Hatfield and S.R. Quake, *Phys. Rev. Lett.* **82**, 3548 (1999).
  - [13] P. Pincus, *Macromolecules* **9**, 386 (1976).
  - [14] R.G. Winkler, *Phys. Rev. Lett.* **82**, 1843 (1999).
  - [15] T.T. Perkins, D.E. Smith, R.G. Larson, and S. Chu, *Science* **268**, 83 (1995).
  - [16] D. Stigter and C. Bustamante, *Biophys. J.* **75**, 1197 (1998).
  - [17] B. Zimm, *Macromolecules* **31**, 6089 (1998).
  - [18] J.F. Marko and E.D. Siggia, *Macromolecules* **28**, 8759 (1995).
  - [19] R.G. Larson, T.T. Perkins, D.E. Smith, and S. Chu, *Phys. Rev. E* **55**, 1794 (1997).
  - [20] S.R. Quake, H. Babcock, and S. Chu, *Nature (London)* **388**, 151 (1997).
  - [21] O.B. Bakajin *et al.*, *Phys. Rev. Lett.* **80**, 2737 (1998).
  - [22] J.C. Meiners and S.R. Quake, *Phys. Rev. Lett.* **82**, 2211 (1999).
  - [23] R.M. Zimmermann and E.C. Cox, *Nucleic Acids Res.* **22**, 492 (1994).
  - [24] M. Doi and S.F. Edwards, *The Theory of Polymer Dynamics* (Clarendon, Oxford, 1989).
  - [25] M.F. Shlesinger, G.M. Zaslavsky, and J. Klafter, *Nature (London)* **363**, 31 (1993).